ChemPubSoc Europe

DOI: 10.1002/chem.201700360

CHEMISTRY A European Journal Full Paper

Gold Complexes

Controlled Interconversion of a Dinuclear Au Species Supported by a Redox-Active Bridging PNP Ligand Facilitates Ligand-to-Gold Electron Transfer

Vincent Vreeken,[a] Maxime A. Siegler,[b] and Jarl Ivar van der Vlugt*[a]

Abstract: Redox non-innocent ligands have recently emerged as interesting tools to obtain new reactivity with a wide variety of metals. However, gold has almost been neglected in this respect. Here, we report mechanistic investigations related to a rare example of ligand-based redox chemistry in the coordination sphere of gold. The dinuclear metal-centered mixed-valent Au^{I}–Au^{III} complex **1**, supported by monoanionic diarylamido-diphosphine ligand PNP^{Pr} and with three chlorido ligands overall, undergoes a complex series of reactions upon halide abstraction by silver salt or Lewis acids such as gallium trichloride. Formation of the ultimate Au^{I}–Au^{I} complex **2** requires the intermediacy of Au^{I}–Au^{I} dimers **5** and **7** as well as the unique Au^{III}–Au^{III} complex **6**, both of which are interconverted in a feedback loop. Finally, unprecedented *ortho*-selective C–H activation of the redox-active PNP ligand results in the carbazolyldiphosphine derivative $PN^{*}P^{Pr}$ via ligand-to-metal two-electron transfer. This work demonstrates that the redox-chemistry of gold may be significantly expanded and modified when using a reactive ligand scaffold.

Introduction

Homogeneous catalysis with well-defined (organometallic) gold complexes has blossomed in the last decade, predominantly with mononuclear Au^{I} species, although dual-gold catalysis with dinuclear Au^{I}–Au^{I} species has also recently been developed.[1] In many cases, halide abstraction using, for example, Ag-salts or Lewis acids, plays a key role in the activation of the gold center for substrate coordination and activation. Metal-centered redox chemistry involving archetypical oxidative addition–reductive elimination processes have recently been demonstrated for a number of supporting ligand types.[2] However, ligand-centered redox-chemistry has been very scarcely reported with gold complexes and so far this has been induced using external oxidants (e.g. H_2O_2 or $PhICl_2$).[3]

Redox-active ligands have recently emerged as interesting tools to obtain new reactivity in homogeneous catalysis.[4,5] Various nitrogen-based ligands (and substrates) have been described as redox non-innocent.[6] For example, tridentate diarylaminophosphino (PNP) ligands engage in reversible one-electron oxidation processes at nitrogen upon deprotonation and coordination of the central amido functionality to a (transition) metal. This is explained by the dominance of the amido p-orbital in the HOMO of these complexes, leading to a large contribution of this orbital in the SOMO of the oxidized complex. Additionally, there is substantial delocalization of the spin density over the phenyl rings of the ligand backbone. As a result, the aromatic rings are susceptible toward radical reactivity at the *ortho*- and *para*-positions with respect to the amido functionality (Scheme 1). Radical addition reactions at the *para*-position are normally irreversible. To date, several examples for PNP oxidation with Mn and Re,[7] Ni[8,9] and Cu[10] have been reported.

Selective *ortho*-reactivity at the PNP-backbone was not reported until our recent publication, which utilized the purple mixed-valent Au^{I}–Au^{III} complex **1** (Scheme 2).[11] This complex is characterized by two distinctly different signals in the ^{31}P NMR spectrum (105.3 for Au^{III}–P and 44.3 ppm for Au^{I}–P). Studying the effect of chloride abstraction, we observed sole formation of the well-characterized product **2** upon addition of two equivalents of $AgNTf_2$ to a solution of **1** (Scheme 2). The backbone of the PNP ligand undergoes a two-electron oxidation concomitant with (at least formally) double C–H activation resulting in the formation of a carbazole moiety. This implies redox reactivity at the two aryl positions *ortho* to the amido substituent, which is in contrast to the previously reported cases of *para*-regioselective oxidative radical reactivity. The overall reaction also involves a two-electron reduction of the Au^{III} center and is therefore redox-neutral.[12]

[a] Dr. V. Vreeken, Dr. Ir. J. I. van der Vlugt
Homogeneous, Supramolecular & Bio-inspired Catalysis
Van 't Hoff Institute for Molecular Sciences, University of Amsterdam
Science Park 904, 1098 XH Amsterdam (the Netherlands)
E-mail: j.i.vandervlugt@uva.nl

[b] Dr. M. A. Siegler
Department of Chemistry, John Hopkins University
Baltimore MD (USA)

Supporting information and the ORCID number(s) for the author(s) of this article can be found under http://dx.doi.org/10.1002/chem.201700360.

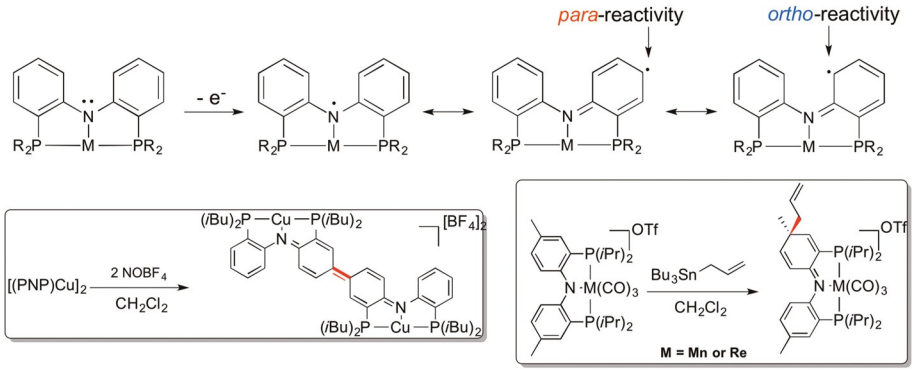

Scheme 1. Oxidation of the PNP scaffold and resulting positions of reactivity.

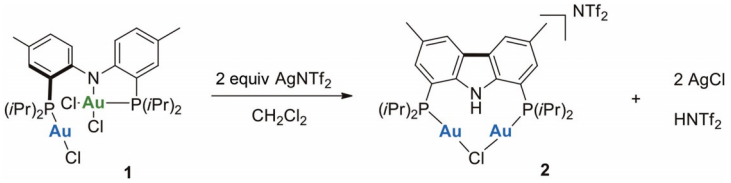

Scheme 2. *Ortho*-reactivity in the PNP ligand backbone by means of oxidative C–C coupling; Au = Au^{I}; Au = Au^{III}.

The unexpected outcome of the described reaction, together with the new redox reactivity displayed by the ligand, warranted a systematic investigation of the transformation. Here, we disclose a detailed investigation and a plausible mechanism for the formation of the intermediates that precede the well-defined formation of **2**, supported by isolation and characterization of various reaction intermediates, and we highlight the role of Ag^{+} in this reaction sequence. The obtained mechanistic insight behind this interesting conversion may lay the foundation for novel redox chemistry and C–H functionalization reactions with Au^{I} and Au^{III}. This paper is structured in the following manner: a) an investigation of the role of Ag-salt, by analyzing products **3** and Tl-analogue **4** formed from the sub-stoichiometric reaction between Au-dimer **1** and Ag-salt (1:0.5 ratio); b) the characterization and inter-dependence of species **5** and **6** formed from an equimolar reaction (1:1 ratio) of Au-dimer:Ag-salt and in the absence of Ag-salt (directly from **3**); c) the conversion of **5** into **6** with the help of a two-electron oxidant, conversion of **6** to final product **2** and the role of **5** and intermediate **7** in this transformation; d) a discussion on the postulated reaction mechanism for C–H activation steps and the overall mechanism for the transformation of Au^{I}–Au^{III} dimer **1** into Au^{I}–Au^{I} dimer **2**.

Results and Discussion

Sub-stoichiometric reaction between Au-dimer 1 and Ag-salt (1:0.5 ratio)

We started our investigation by considering the possible role of Ag^{+} in the reaction, either as a chemical oxidant to initiate (ligand-based) reactivity or as a halide-abstracting agent. Given that the reaction works equally well using two equivalents of non-oxidizing $GaCl_3$, and that the cyclic voltammogram of **1** shows an irreversible oxidation event at 0.79 V vs. Fc/Fc^{+} (well above the oxidation potential of Ag^{+} in CH_2Cl_2; Fc = ferrocene),[13] the possibility of Ag^{+} acting as an oxidant was discarded. Addition of 0.5 equiv of $AgNTf_2$ (Tf = trifluoromethanesulfonyl) to **1** almost instantaneously resulted in a dark blue-colored mixture but attempts to cleanly isolate the anticipated dimeric product **3** were unsuccessful. The mass spectrum of the crude mixture contained a signal matching the species $[(\mathbf{1})_2{\subset}Ag]^{+}$ (*m/z*: found 1965.1010, calculated 1965.1082). Full conversion of the starting material was observed in the ^{31}P NMR spectrum, with the Au^{I}–P signal unaffected, whereas the Au^{III}–P signal shifted downfield (to 111.0 ppm; see the Supporting Information).

To elucidate the role of Ag^{+} in this reaction, we performed the same reaction using $TlPF_6$. Contrary to our expectations, addition of 2 equiv of $TlPF_6$ did not generate **2** but instead formed the new well-defined complex **4**. The same product was formed quantitatively when one or even half a molar equivalent of $TlPF_6$ was used. In line with this, we were able to generate **4** in 92% yield using only 0.5 molar equiv of $TlPF_6$ in the reaction. The generation of **4** is also accompanied by a color change from purple to dark blue. UV/Vis spectroscopy shows a small red-shift of the absorption bands compared to the starting material **1** and roughly doubling of the extinction coefficients. The ^{31}P NMR spectrum of **4** shows a signal at 110.1 ppm, indicating that the P-atom coordinated to a Au^{III} center is only subtly affected ($\Delta\delta = +4.8$ ppm vs. **1**) by the reaction and no reduction of this metal center has taken place. The signal at 44.3 ppm does not shift compared to the starting material and the ^{1}H NMR spectrum of product **4** displays only minor differences from that of **1**. Similar to the spectrum of the starting material, a very upfield-shifted aromatic signal ($\delta =$ 5.83 ppm) is observed, which is attributed to shielding effects by the adjacent phenyl ring. These findings indicate that the structural integrity of the starting material is preserved upon reaction with Tl^{+}. Interestingly, ESI-MS data of product **4** suggested incorporation of thallium into complex **1** in a 1:2 ratio ($TlPF_6$:**1**) to give $[(\mathbf{1})_2{\subset}Tl]^{+}$ (Scheme 3).

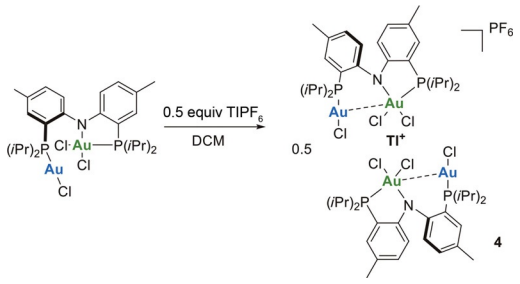

Scheme 3. Schematic representation of Tl^+ scavenging by **1** to generate complex **4**, $[(1)_2 \subset Tl]^+$; Au = Au^I; Au = Au^{III}.

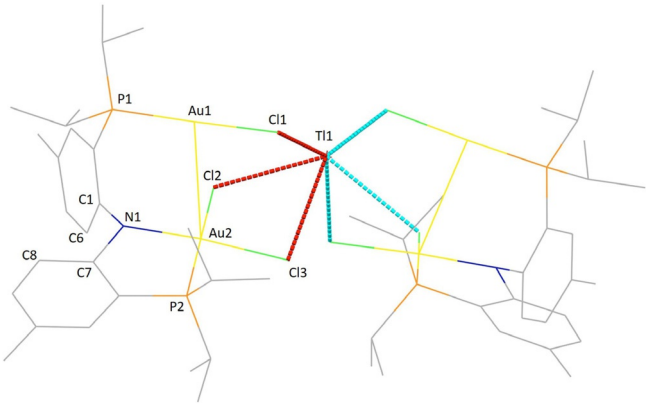

Figure 1. Preliminary connectivity plot for **4**. Approximate bond lengths (Å) and angles (°): Au1–Au2 3.19; P1–Au1 2.25; Au1–Cl1 2.31; P2–Au2 2.26; N1–Au2 2.02; Au2–Cl2 2.31; Au2–Cl3 2.38; Cl1–Tl1 3.27; Cl2–Tl1 3.10; Cl3–Tl1 3.11; P1-Au1-Cl1 178.2; N1-Au2-Cl2 174.1; P2-Au2-Cl3 173.0; C1-C6-C7-C8 77.

X-ray diffraction from single crystals grown from a CH_2Cl_2/pentane solution did not provide high enough data quality for full refinement, but we are confident that the model resulting in the preliminary connectivity plot (Figure 1) for complex **4** is correct. This species can be described as a dimeric complex, in which the Tl^+ ion is uniquely sandwiched between the chlorido ligands of two digold complexes **1**. The distances between the Tl^+ core and the chloride atoms coordinated to the Au^{III} center are approximately 3.10 Å, indicating non-covalent interactions that likely cause the downfield shift of the Au^{III}–P signal in the ^{31}P NMR spectrum. The longer Cl1–Tl distance of about 3.27 Å may also still allow for a weak interaction. However, it is possible that this interaction is only present in the solid state, as no ^{31}P NMR shift was observed for the P(Au^I) donor. The approximate Au^I–Au^{III} distance of 3.19 Å supports a d^8–d^{10} interaction in **4**, whereas this is absent in **1**, but this is likely due to a different orientation of the Au^I center in the solid state. Given that incorporation of Ag^+ in gold complexes through non-covalent interactions has been reported,[14,15] that silver ions may affect gold catalysis,[16] and the analogy between 0.5 equiv Ag^+ vs. Tl^+, we propose that **3** is the first intermediate in the reaction from **1** to **2** (Scheme 4).

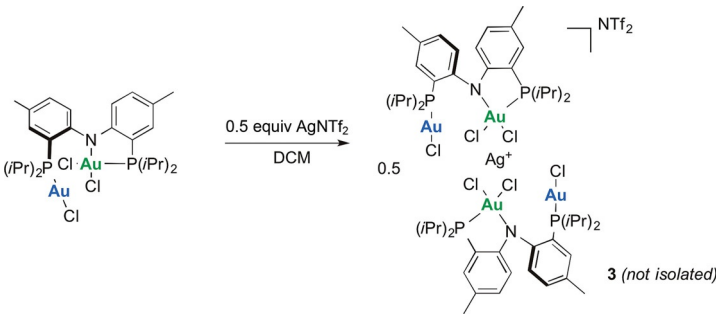

Scheme 4. Proposed formation of dimeric species **3** by reaction of **1** with $AgNTf_2$ (2:1 ratio); Au = Au^I; Au = Au^{III}.

Stoichiometric reaction between Au-dimer 1 and Ag-salt (1:1 ratio)

The addition of an equimolar amount of $AgNTf_2$ to **1** generates a mixture of products, as evidenced by ^1H (Figure 2) and

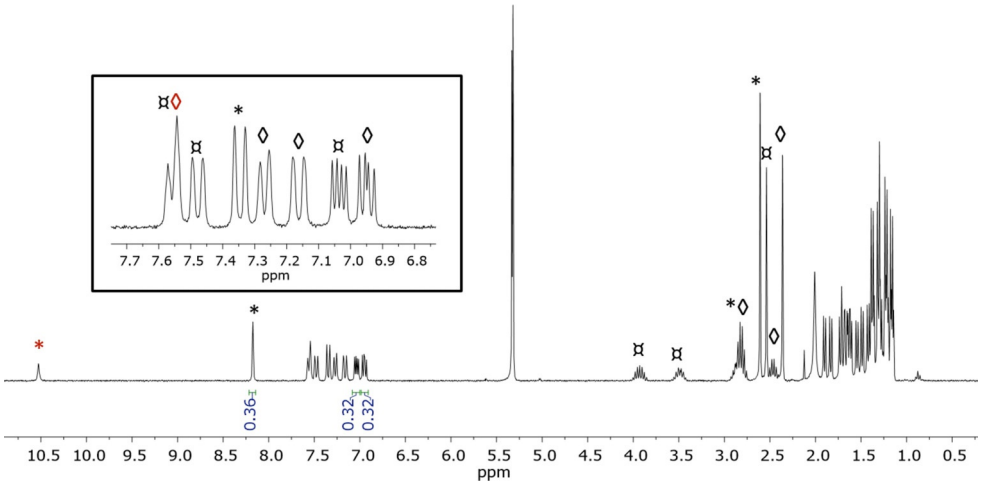

Figure 2. ^1H NMR spectrum of product mixture of the reaction between $AgNTf_2$ and **1** (1:1 ratio in CD_2Cl_2). Assignment of peaks for **2** (*), **5** (◇) and **6** (¤); red color for N–H.

^{31}P NMR spectroscopy. Analysis of the spectra showed the presence of final carbazole-based product **2** (^{31}P NMR: 40.3 ppm) and two other species **5** and **6** in a 1:1:1 ratio, with no trace of species **3**. Complex **5** (^{31}P NMR: singlet at 40.5 ppm) can be identified as dinuclear complex [(PNP)Au$_2$(μ-Cl)]NTf$_2$, which we previously prepared from an independent synthesis.[11] Its formation in the current reaction with Ag-salt implies a two-electron reduction of the Au^{III} center and reprotonation of the central amide, but no ligand backbone oxidation. Compound **6** shows one singlet at 102.1 ppm in the ^{31}P NMR spectrum, suggestive of an overall C_2 symmetry and the presence of Au^{III}-phosphine units. The ^{1}H NMR spectrum reveals an intact ligand backbone with three signals for the six tolyl hydrogen atoms, supporting the C_2 symmetric nature of the molecule.

Yellow-orange single crystals of **6** suitable for X-ray structure determination were obtained from CH_2Cl_2/toluene. Consistent with the NMR data, the obtained symmetric structure contains two square planar Au^{III} centers (Figure 3). Both gold centers are

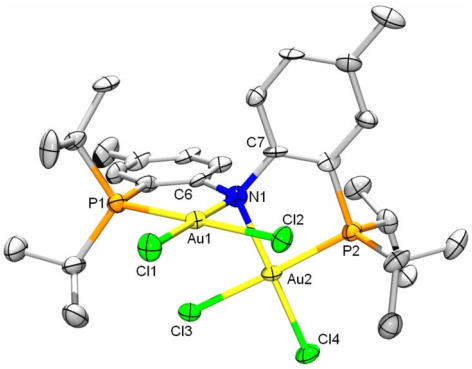

Figure 3. Displacement ellipsoid plot (50% probability level) for **6**. Hydrogen atoms and NTf$_2$ counterion are omitted for clarity, selected bond lengths (Å) and angles (°) given for one crystallographically independent molecule: Au1–Au2 3.2484(5); N1–Au1 2.127(8); Au1–Cl1 2.273(2); Au1–Cl2 2.340(2); P1–Au1 2.291(2); N1–Au2 2.114(8); Au2–Cl3 2.339(2); Au2–Cl4 2.276(2); P2–Au2 2.288(2); C7-N1-C6 111.6(6); C7-N1-Au2 112.7(5); Au1-N1-C6 113.2(6); Au1-N1-Au2 100.0(3); N1-Au1-Cl1 179.1(2); P1-Au1-Cl2 177.62(9); N1-Au2-Cl4 178.7(2); P2-Au2-Cl3 177.67(9); C5-C6-C7-C8 93.6(8).

coordinated to the central bridging amido unit of the PNP ligand, as well as to one P-atom and two chloride ligands. The backbone of the ligand is severely twisted (∢C5-C6-C7-C8 93.6(8)–94.0(9)), leading to an almost orthogonal arrangement of the two phenyl rings. The nature of compound **6** was further confirmed by HR-MS. The overall structure of **6** implies a two-electron oxidation with respect to the starting compound **1**. The overall reaction in Scheme 5 is redox-neutral given that a two-electron reduction is required to co-generate **5**.

Generation of complexes 5 and 6 from 3 without Ag-salt

The presence of both species **5** and **6** in the product mixture signifies extensive charge-transfer. Furthermore, reprotonation of the amido functionality in **5** suggests that this overall reaction is acid-induced. To test this hypothesis, we exposed in situ

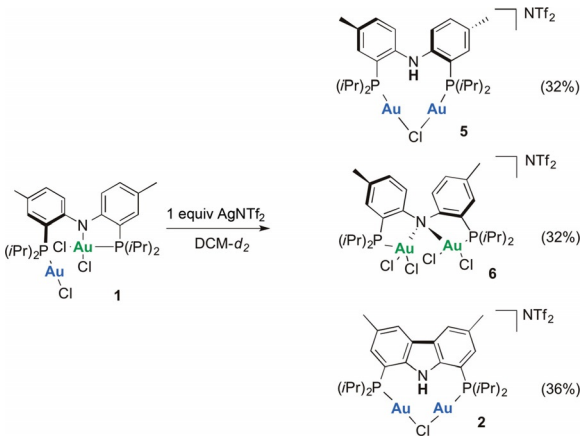

Scheme 5. The equimolar reaction of **1** with AgNTf$_2$ produces **2**, **5**, and **6** in a 1:1:1 ratio (by NMR spectroscopy); Au = Au^{I}; Au = Au^{III}.

generated complex **3** to an equimolar amount of HBF$_4$, which resulted in a mixture of **5** and **6** (Scheme 6). Treatment of Tl-complex **4** with HBF$_4$ also led to both dinuclear complexes, albeit less cleanly. These results demonstrate that the acid-induced redox-reaction to form both a Au^{I}–Au^{I} and a Au^{III}–Au^{III} species is a viable second step in the formation of carbazole product **2**. We suggest that the required acid to allow for this step is formed at the end of the total reaction.

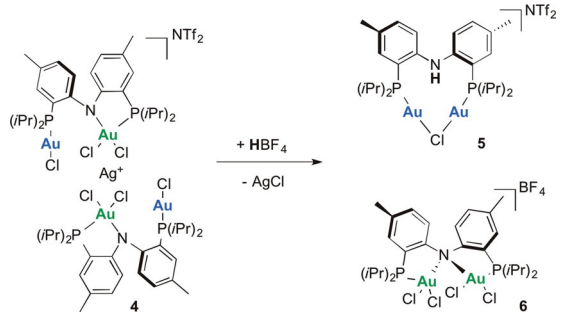

Scheme 6. Reaction of assembly **3** with HBF$_4$; assignment of counter-anions BF$_4$ and NTf$_2$ is arbitrary.

Conversion of 5 into 6 with a two-electron oxidant

The oxidation states of the gold centers in the series **5**–**1**–**6** increase stepwise from Au^{I}–Au^{I} to Au^{I}–Au^{III} to Au^{III}–Au^{III} and the complexes are stabilized by either a neutral (protonated) or monoanionic (deprotonated) PNP ligand. However, Au^{I}–Au^{III} species **1** is not cleanly converted with 1 equiv of the two-electron oxidant dichloro-λ^3-(iodanyl)benzene PhICl$_2$ to generate **6Cl** as an analogue of **6** (with Cl$^-$ as counterion). Rather, this reaction led to a mixture of products, with **6** present only as a minor species (< 10%, determined by ^{31}P NMR spectroscopy). Species **1** was previously generated from Au^{I}–Au^{I} precursor Cl-Au-(κ^1:*P*-PNP-κ^1:*P*)-Au-Cl with 1 equiv of PhICl$_2$, under expulsion of HCl. We therefore sought to elucidate if the reactivity of **5** toward the same oxidant would also generate species **1** (with formation of HNTf$_2$). However, reaction of **5** with an equimolar

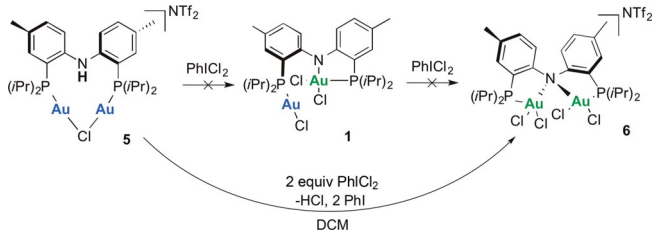

Scheme 7. Reactivity scheme to convert complexes **5** and **1** into **6** (or **6Cl**) with $PhICl_2$; Au = Au^{I}; Au = Au^{III}.

amount of $PhICl_2$ instead leads to a 1:1 mixture of the starting material and **6** (Scheme 7), suggesting the intermediacy of a compound with either a lower oxidation potential than the starting material or with the tendency to disproportionate into **5** and **6**. Reaction of two equivalents of $PhICl_2$ with **5** led to full conversion to **6**. The nature of the liberated acid (HCl vs. $HNTf_2$) may also be important in this regard.

Initial insight into the conversion of 6 to final product 2

Having established the co-dependence of the observed intermediates **5** and **6** in this overall reaction, the formation of the final carbazole product **2** was investigated. Full conversion of a 1:1 mixture of **5** and **6** to complex **2** was observed upon addition of 3 equiv of $AgNTf_2$, confirming the importance of both intermediates in the formation of **2**. Without addition of $AgNTf_2$, a mixture of compounds **5** and **6** is completely stable and both species do not react together. We assume that complex **6** is the most likely precursor to final carbazole product **2** because its high oxidation state and potentially strongly oxidizing character may invoke a two-electron oxidation of the ligand backbone. This conversion is accompanied by formal release of HCl and a two-electron reduction of the complex. It should therefore be triggered by addition of a suitable two-electron reductant to complex **6**. Treatment of **6** with $AgNTf_2$ did not result in appreciable conversion to **2** (< 5%), although NMR spectra do indicate interaction of the silver salt with the complex. Reaction of **6** with $Pd^{0}(dba)_2$ (dba = dibenzylideneacetone) as a two-electron reductant in the absence of $AgNTf_2$ also gives no conversion. However, in the presence of both $AgNTf_2$ and $Pd^{0}(dba)_2$, **6** is quantitatively transformed to **2**, as indicated by NMR spectroscopy and mass spectrometry (Scheme 8).

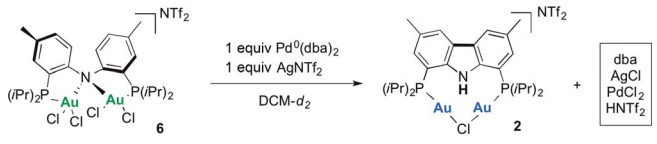

Scheme 8. Reaction of complex **6** with $Pd^{0}(dba)_2$ as a sacrificial two-electron reducing agent to form **2**, in the presence of $AgNTf_2$. By-products listed in box were not quantified. Au = Au^{I}; Au = Au^{III}.

Role of 5 in the conversion of 6 to final product 2 through formation of intermediate 7

Subsequently, we considered the role of **5** in the overall conversion scheme. With **6** being the proposed precursor to the final product, complex **5** has to be fully converted to this species to reach the observed yields of the scrutinized reaction (68% after crystallization). Therefore, we initially speculated that **5** could function as the two-electron reducing agent that is required for **6** to react. However, the presence of both complexes in stable product mixtures excludes this option. As an alternative, the presence of large amounts of silver salt can lead to halide abstraction to form a "*pseudo*-dicationic" Au_2-complex, possibly more prone to act as a reductant than **5**. Reaction of compound **5** with $AgNTf_2$ indeed results in the formation of dicationic complex **7** (Scheme 9). Weak coordination of the NTf_2 anions to the gold centers is manifested by a small shift in the ^{19}F NMR spectrum compared to **5** (−75.9 ppm for **7** vs. −79.5 ppm for **5**). Compound **7** can be independently prepared by treatment of the parent $(PNP)Au_2Cl_2$ complex with 2 equiv of $AgNTf_2$. Reactivity studies show that addition of an equimolar amount of HCl (0.1 M solution in water) to **7** regenerates **5**. Reaction of **7** with 2 equiv of $PhICl_2$ leads to quantitative formation of **6**. The coordination of the triflamide units to gold was corroborated by single crystal X-ray crystallography (Figure 4).

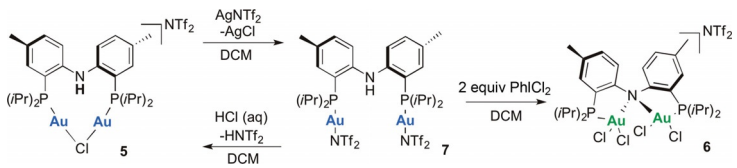

Scheme 9. Interconversion between species **5** and **7** with $AgNTf_2$ or HCl and preparation of species **6** from **7** by two-electron oxidation using $PhICl_2$; Au = Au^{I}; Au = Au^{III}.

To further support our hypothesis that a "*pseudo*-dicationic" Au_2-complex is required to convert **6**, the reactivity of Au^{III}–Au^{III} dimer **6** with **7** was investigated by preparation of a 1:1 mix-

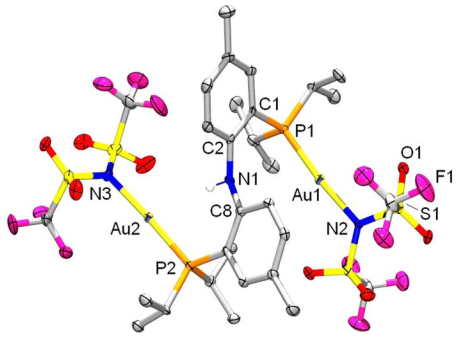

Figure 4. Displacement ellipsoid plot (50% probability level) for **7**. Hydrogen atoms and disordered pentane lattice solvent are omitted for clarity. Selected bond lengths (Å) and angles (°): P1–Au1 2.2378(12); Au1–N2 2.1189(39); P2–Au2 2.2362(13); Au2–N3 2.1120(41); N2-Au1-P1 174.40(13); N3-Au2-P2 176.67(15).

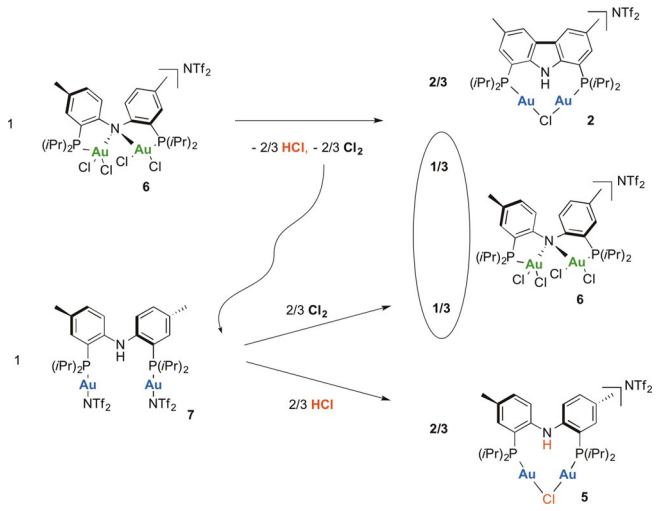

Scheme 10. Schematic representation of the reaction of complex **6** with **7** and a proposal for the observed ratio of products; Au = Au^{I}; Au = Au^{III}.

ture of these compounds in dichloromethane. Analysis of the reaction mixture by NMR spectroscopy reveals the presence of the carbazole product **2** and complexes **5** and **6** in equal amounts, whereas species **7** is fully consumed. The observed product ratio is in line with the expected values (Scheme 10). Thus, complex **7** serves both as a two-electron reductant to form **6** and as an HCl scavenger to produce **5**. This implies that only two-thirds of **6** can react to form product **2** before **7** is completely converted and the reaction comes to a halt. This experiment shows that halide abstracting agents are not directly involved to form **2**, but rather facilitate the formation of compounds able to react with precursor **6**.

Overall mechanism for the transformation of Au^{I}–Au^{III} dimer 1 into Au^{I}–Au^{I} dimer 2

The combined findings described in the previous subsections lead to the following mechanistic proposal for the investigated reaction (Scheme 11). Initial scavenging of one Ag^{+} cation by 2 equiv of Au^{I}–Au^{III} complex **1** generates adduct **3**. This intermediate undergoes an acid-induced reorganization reaction, as supported by a stoichiometric reaction with HBF_4. Given that no external Brønsted acid is added to the reaction, we propose that reorganization in the original sequence is initiated by trace amounts present in the solvent. This reorganization produces Au^{I}–Au^{I} complex **5** and Au^{III}–Au^{III} complex **6**. The former reacts with $AgNTf_2$ to form **7** by salt metathesis. Stoichiometric reaction of **7** with **6** converts this Au^{III}–Au^{III} dimer to Au^{I}-dimer **2** by formal ligand-to-gold electron transfer, concomitant with oxidative C–C bond formation on the redox-active ligand fragment, possibly by formation of an *ortho*-phenyl radical.[17] The released HCl and two-electron oxidation equivalents (denoted as 'Cl_2') react with **7** to regenerate complexes **5** and **6** in a 2:1 ratio, concomitant with $HNTf_2$. This acid can drive the disproportionation reaction to completion. A total of 2 equiv of $AgNTf_2$ is required to drive the overall reaction to full conversion.

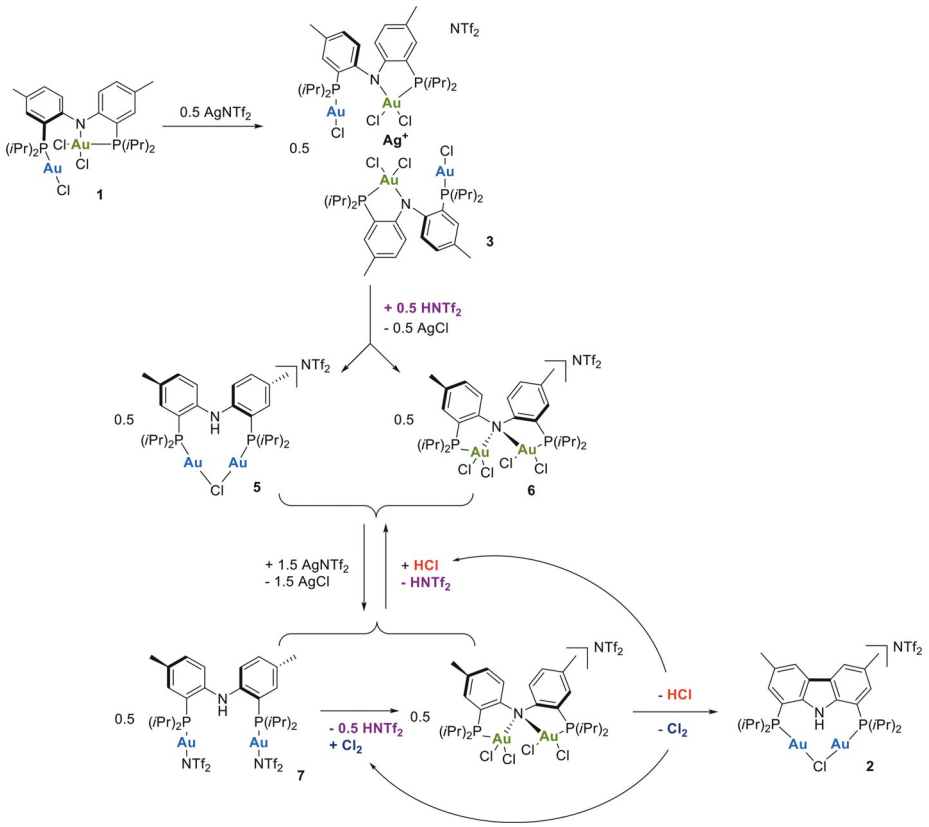

Scheme 11. Postulated mechanism, including feedback loop involving species **7**, for the overall formation of **2** from reaction of **1** with $AgNTf_2$; Au = Au^{I}; Au = Au^{III}.

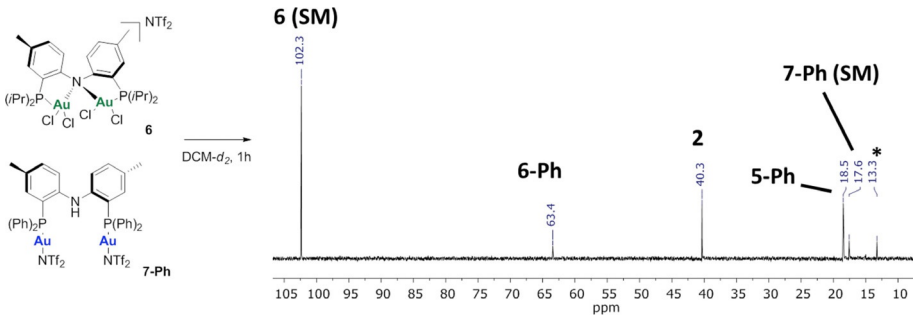

Figure 5. ^{31}P NMR spectrum of product mixture after reacting **6** and **7-Ph** for 1 h; * is putatively assigned to **2-Ph**.

Cross-over experiments were conducted to find further proof for the proposed pathway. For this purpose $Au_2(NTf_2)_2(^{Ph}PNP^{Ph})$ **7-Ph** was prepared using the same route as that used for the bis(isopropyl)phosphine congener **7**. Mixing this complex with **6** initially led to exclusive (but incomplete) conversion of the latter to product **2**, whereas some formation of **5-Ph**, **6-Ph**, and **2-Ph** was also observed in the NMR spectra (Figure 5). After prolonged reaction time, however, almost full consumption of **6** was observed in the NMR spectra, accompanied by generation of **6-Ph** and **5**, demonstrating a feedback-loop-like process with these structural isomers.

Conclusion

We have presented a mechanistic investigation of the reaction of mixed-valent Au^I–Au^{III} complex **1** with $AgNTf_2$ to generate Au^I–Au^I **2**, featuring unprecedented *ortho*-C–H backbone oxidation of the redox-active *o*-ditolylamino-diphosphine PNP ligand, with formation of a carbazole framework. The isolation and characterization of unique dinuclear gold intermediate complexes allows for the formulation of a plausible reaction mechanism. We propose that Ag^+ ions primarily act as a halide-abstracting agent during the reaction. Initial scavenging of Ag^+ by two species of **1** is followed by an acid-induced disproportionation reaction, resulting in Au^I–Au^I compound **5** and novel Au^{III}–Au^{III} compound **6**. Bridging chloride abstraction from **5** generates **7**, which functions both as an HCl scavenger and as a reductant, allowing for the conversion of **6** to final product **2**. Cross-over experiments and the use of $Pd(dba)_2$ as an alternative reductant confirm that **6** should be regarded as the precursor to **2**. We speculate that the exhibited *ortho*-reactivity of the ligand backbone arises from a combination of steric preorganization and stepwise oxidation of the ligand by the gold centers. The range of oxidation states of the isolated structures, from Au^I–Au^I to Au^{III}–Au^{III}, highlights the versatility of the PNP ligand. The central amine functionality of the PNP ligand seems to be essential for the stabilization of the complexes in higher oxidation states, while it also allows for Au^I–Au^I structures. The isolation of Tl-adduct **4** and the proposed intermediacy of Ag-congener **3** show that halide abstracting agents are not, by definition, innocent and that their incorporation into partly stable complexes should be considered. Furthermore, this work demonstrates that the growing field of elementary reactions and redox chemistry with gold may also entail ligand reactivity, including C–H activation. Although strictly stoichiometric at present, such reactivity may eventually significantly broaden the scope for future developments in the field of (dinuclear) gold catalysis.

Experimental Section

General Methods

With exception of the compounds given below, all reagents were purchased from commercial suppliers and used without further purification. PN^HP^{iPr} (bis(2-diisopropylphosphino-4-methylphenyl)-amine),[18] PN^HP^{Ph} (bis(2-diphenylphosphine-4-methylphenyl)-amine),[19] and $PhICl_2$[20] were synthesized according to literature procedures. Compounds **1**, **5**, and $(PN^HP^{iPr})Au_2Cl_2$ were previously reported by us.[11] Toluene, tetrahydrofuran and pentane were distilled from sodium benzophenone ketyl. CH_2Cl_2 was distilled from CaH_2. NMR spectra (^1H, $^1H\{^{31}P\}$, $^{13}C\{^1H\}$, ^{19}F, $^{31}P\{^1H\}$) were measured on a Bruker DRX 500, Bruker AV 400, Bruker DRX 300, or on a Bruker AV 300 spectrometer at room temperature, unless noted otherwise. High resolution mass spectra were recorded on a JEOL AccuTOF LC, JMS-T100LP mass spectrometer using cold spray ionization (CSI) and electron spray ionization (ESI) and on a JEOL AccuTOF GC v 4 g, JMS-T100GCV mass spectrometer using field desorption (FD). UV/Vis spectra were recorded on a Hewlett–Packard 8453 spectrophotometer. Elemental analysis was carried out by Kolbe Mikroanalytisches Laboratorium, Mülheim, Germany.

Complex $PN^HP^{Ph}Au_2Cl_2$. A flame-dried Schlenk under N_2-atmosphere was charged with a CH_2Cl_2 solution (5 mL) of PN^HP^{Ph} (139 mg, 0.25 mmol). To this colorless solution was added $AuCl(SMe)_2$ (147 mg, 0.50 mmol), leading to the formation of a white solid. The suspension was stirred overnight before pentane (10 mL) was added. The solid was allowed to settle and the supernatant was removed. The product ($PN^HP^{Ph}Au_2Cl_2$) was dried in vacuo to give a white powder (194 mg, 75% yield). The product proved to be barely soluble in common NMR solvents, hindering complete spectroscopic characterization. ^1H NMR (400 MHz, CD_2Cl_2): $\delta = 7.59$–7.36 (m, 17H), 7.28 (d, $J = 8.5$ Hz, 2H), 7.25–7.16 (m, 3H), 7.15–7.08 (m, 2H), 6.42 (d, $J = 12.7$ Hz, 2H), 5.82 (s, 1H), 2.14 ppm (s, 6H); $^{31}P\{^1H\}$ NMR (162 MHz, CD_2Cl_2): $\delta = 19.6$ ppm (s); HR-MS (ESI) calcd for $[M-Cl]^+$ $C_{38}H_{33}Au_2ClNP_2$ *m/z*: 994.1108, found 994.1135.

Complex 4: A flame-dried Schlenk under argon atmosphere was loaded with **1** (33 mg, 0.0355 mmol) and $TlPF_6$ (6.2 mg, 0.0177 mmol) before addition of CH_2Cl_2 (1.5 mL), which instantaneously led to a dark blue solution. After stirring for 3 h, the solution

was filtered and then concentrated to about 0.5 mL. Subsequent addition of pentane led to precipitation of a dark blue solid. The supernatant was removed and the residue was dried to yield product **4** (36 mg, 92%). Single crystals suitable for X-ray diffraction were grown from DCM/pentane. ^{1}H NMR (400 MHz, CD_2Cl_2): $\delta =$ 7.46 (d, $J=8.0$ Hz, 1H), 7.24 (d, $J=8.7$ Hz, 1H), 7.11 (dd, $J=8.1$, 4.7 Hz, 1H), 7.00 (d, $J=8.8$ Hz, 1H), 6.95 (d, $J=10.8$ Hz, 1H), 5.83 (dd, $J=8.7$, 4.8 Hz, 1H), 3.37–3.23 (m, 1H), 3.12–3.00 (m, 1H), 2.86–2.71 (m, 1H), 2.47 (s, 3H), 2.25 (s, 3H), 2.09–1.95 (m, 1H), 1.71 (dd, $J=19.4$, 7.0 Hz, 3H), 1.60 (dd, $J=20.4$, 7.0 Hz, 3H), 1.52–1.25 (m, 12H), 1.14 (dd, $J=18.5$, 7.3 Hz, 3H), 1.02 ppm (dd, $J=16.3$, 7.2 Hz, 3H); ^{31}P{^{1}H} NMR (162 MHz, CD_2Cl_2): $\delta=110.1$ (s), 44.3 (s), −144.5 ppm (hept, $J=711.1$ Hz); ^{13}C{^{1}H} NMR (126 MHz, CD_2Cl_2): $\delta=165.2$ (d, $J=11.0$ Hz), 152.7 (d, $J=6.0$ Hz), 138.0 (d, $J=7.6$ Hz), 136.7 (d, $J=2.9$ Hz), 134.5 (d, $J=2.0$ Hz), 133.4 (d, $J=6.0$ Hz), 132.5 (d, $J=2.9$ Hz), 131.7 (d, $J=2.3$ Hz), 131.6 (d, $J=9.7$ Hz), 126.6 (d, $J=55.3$ Hz), 116.8 (d, $J=13.2$ Hz), 104.3 (d, $J=58.3$ Hz), 29.3 (d, $J=28.1$ Hz), 29.1 (d, $J=34.0$ Hz), 26.5 (d, $J=33.2$ Hz), 23.8 (d, $J=33.0$ Hz), 21.6 (s), 21.4 (d, $J=4.2$ Hz), 20.8 (d, $J=3.6$ Hz), 20.2 (s), 19.5 (d, $J=4.1$ Hz), 18.5 (d, $J=56.7$ Hz), 18.0 (d, $J=70.6$ Hz), 17.6 ppm (d, $J=3.7$ Hz); UV/Vis: λ_{max} (ε) = 278 nm (22.8×10^3 м$^{-1}$ cm^{-1}), 354 nm (14.3×10^3 м$^{-1}$ cm^{-1}), 593 nm (2.4×10^3 м$^{-1}$ cm^{-1}); HR-MS (ESI) calcd for $[M-PF_6]^+$ $C_{52}H_{80}Au_4Cl_6N_2P_4TL$ *m/z*: 2061.1776, found 2061.1802; elemental analysis calcd for $C_{52}H_{80}Au_4Cl_6F_6N_2P_5TI$: C 28.30, H 3.65, N 1.27; found C 28.31, H 3.85, N 1.23.

Complex 5-Ph: A vial was charged with **PN^{H}P^{Ph}**Au_2Cl_2 (50.2 mg, 0.05 mmol) and $AgNTf_2$ (19.4 mg, 0.05 mmol). Then, 5 mL CH_2Cl_2 was added and the resulting suspension was stirred for 45 minutes during which time it slightly colored purple. The mixture was then filtered over Celite. The colorless filtrate was then dried under removed pressure, yielding the product (**5-Ph**) as an off-white solid (52 mg, 82%). ^{1}H NMR (300 MHz, CD_2Cl_2): $\delta=7.74$–7.39 (m, 20H), 7.10 (d, $J=8.5$ Hz, 2H), 7.05 (s, 1H), 6.59–6.42 (m, 4H), 2.12 ppm (s, 6H); ^{31}P{^{1}H} NMR (162 MHz, CD_2Cl_2): $\delta=18.5$ ppm (s); ^{13}C{^{1}H} NMR (126 MHz, CD_2Cl_2): $\delta=144.1$ (d, $J=7.6$ Hz), 135.2 (d, $J=2.4$ Hz), 134.8 (t, $J=13.7$ Hz), 134.2 (s), 134.2 (s), 134.1 (s), 133.8 (s), 133.4 (s), 126.3 (s), 125.8 (s), 125.3 (s), 122.4 (d, $J=6.7$ Hz), 120.3 (q, $J=321.7$ Hz), 118.0 (s), 117.5 (s), 20.8 ppm (s); ^{19}F NMR (282 MHz, CD_2Cl_2): $\delta=-79.5$ ppm (s); HR-MS (ESI) calcd for $[M-NTf_2]^+$ $C_{38}H_{33}Au_2ClNP_2$ *m/z*: 994.1108, found 994.1120.

Complex 6: A solution of **5** (55 mg, 0.05 mmol) in 2 mL CH_2Cl_2 was prepared in a vial. To the colorless mixture was added $PhICl_2$ (27 mg, 0.10 mmol) as a solid, causing an immediate color change to yellow. The resulting mixture was stirred for 45 minutes. Then, pentane was added resulting in the precipitation of a yellow solid. The supernatant was removed and the yellow product was dried. The crude product could be recrystallized from CH_2Cl_2/pentane resulting in yellow/orange crystals (58 mg, 96%). Crystals suitable for X-ray analysis were grown from CH_2Cl_2/toluene. ^{1}H NMR (400 MHz, CD_2Cl_2): $\delta=7.56$ (d, $J=8.5$ Hz, 2H), 7.47 (d, $J=9.6$ Hz, 2H), 7.04 (dd, $J=8.7$, 4.5 Hz, 2H), 3.94 (hept, $J=7.4$ Hz, 2H), 3.56–3.41 (m, 2H), 2.54 (s, 6H), 1.87 (dd, $J=20.3$, 7.2 Hz, 6H), 1.74–1.54 ppm (m, 18H); ^{31}P{^{1}H} NMR (162 MHz, CD_2Cl_2): $\delta=102.1$ ppm (s); ^{13}C{^{1}H} NMR (101 MHz, CD_2Cl_2): $\delta=158.4$ (d, $J=8.0$ Hz), 142.3 (d, $J=8.2$ Hz), 138.0 (d, $J=2.7$ Hz), 133.6 (d, $J=1.6$ Hz), 128.5 (d, $J=10.7$ Hz), 121.1 (d, $J=51.0$ Hz), 119.8 (q, $J=321.4$ Hz), 35.9 (d, $J=25.1$ Hz), 29.8 (d, $J=28.0$ Hz), 21.2 (d, $J=5.6$ Hz), 20.5 (s), 19.9 (s), 18.9 (d, $J=2.1$ Hz), 18.6 ppm (d, $J=4.6$ Hz); UV/Vis: λ_{max} (ε) = 334 nm (9.1×10^3 м$^{-1}$ cm^{-1}), 385 nm (*shoulder*, 5.2×10^3 м$^{-1}$ cm^{-1}); HR-MS (ESI) calcd for $[M-NTf_2]^+$ $C_{26}H_{40}Au_2Cl_4NP_2$ *m/z*: 964.0695, found 964.0676; elemental analysis calcd for $C_{28}H_{40}Au_2Cl_4F_6N_2O_4P_2S_2$: C 27.03, H 3.24, N 2.25; found C 27.37, H 3.86, N 2.02.

Complex 6-Ph: A vial was charged with **5-Ph** (25.5 mg, 0.02 mmol) dissolved in 1 mL CH_2Cl_2. While stirring the colorless solution, $PhICl_2$ (11.0 mg, 0.04 mmol) was added as a solid. The resulting yellow mixture was stirred for 45 min. Then pentane was added, which resulted in the precipitation of a solid. The supernatant was removed and the product was evaporated to dryness, yielding a yellow solid (25 mg, 90%). ^{1}H NMR (400 MHz, CD_2Cl_2): $\delta=8.06$ (dd, $J=15.0$, 7.8 Hz, 4H), 7.98–7.85 (m, 8H), 7.82–7.75 (m, 4H), 7.73–7.65 (m, 4H), 7.44 (d, $J=12.3$ Hz, 2H), 7.39 (d, $J=8.9$ Hz, 2H), 6.71 (dd, $J=8.5$, 5.2 Hz, 2H), 2.45 ppm (s, 6H); ^{31}P{^{1}H} NMR (162 MHz, CD_2Cl_2): $\delta=63.3$ ppm (s); ^{13}C{^{1}H} NMR (101 MHz, CD_2Cl_2): $\delta=156.1$ (d, $J=12.2$ Hz), 143.8 (d, $J=9.2$ Hz), 139.6 (s), 136.6 (d, $J=3.3$ Hz), 136.4 (s), 136.3 (s), 136.3 (s), 134.7 (d, $J=11.1$ Hz), 134.1 (s), 131.3 (d, $J=13.2$ Hz), 130.3 (d, $J=14.4$ Hz), 128.3 (d, $J=12.1$ Hz), 123.1 (d, $J=5.2$ Hz), 122.4 (d, $J=2.0$ Hz), 121.3 (s), 120.5 (s), 120.3 (q, $J=323.2$ Hz), 20.81 ppm (s); HR-MS (ESI) calcd for $[M-NTf_2]^+$ $C_{38}H_{32}Au_2Cl_4NP_2$ *m/z*: 1098.0095, found 1098.0113.

Complex 7: A vial was loaded with **(PN^{H}P^{iPr})**Au_2Cl_2 (89 mg, 0.1 mmol) and $AgNTf_2$ (78 mg, 0.2 mmol), then 5 mL CH_2Cl_2 was added. The resulting mixture was stirred for 1.5 h. Subsequently, it was filtered over Celite and the volatiles were removed under reduced pressure. The slightly purple crude product (113 mg, 82%) was recrystallized from a CH_2Cl_2/pentane mixture, leading to colorless crystals (78 mg, 56%). ^{1}H NMR (400 MHz, CD_2Cl_2): $\delta=7.32$–7.25 (m, 4H), 6.83 (dd, $J=8.2$, 5.2 Hz, 2H), 6.39 (s, 1H), 2.78 (dp, $J=10.2$, 6.8 Hz, 2H), 2.45 (h, $J=7.2$ Hz, 2H), 2.36 (s, 6H), 1.41 (dd, $J=19.5$, 6.7 Hz, 6H), 1.32–1.17 ppm (m, 18H); ^{31}P{^{1}H} NMR (162 MHz, CD_2Cl_2): $\delta=42.9$ ppm (s); ^{13}C{^{1}H} NMR (101 MHz, CD_2Cl_2): $\delta=147.4$ (d, $J=5.7$ Hz), 135.0 (d, $J=2.3$ Hz), 134.5 (d, $J=9.2$ Hz), 134.1 (s), 126.2 (s), 119.6 (q, $J=323.1$ Hz), 115.7 (d, $J=56.7$ Hz), 28.5 (d, $J=35.9$ Hz), 24.3 (d, $J=37.7$ Hz), 21.0 (s), 20.6 (d, $J=2.5$ Hz), 20.3 (d, $J=5.6$ Hz), 19.3 (s), 18.88 ppm (s); ^{19}F NMR (282 MHz, CD_2Cl_2): $\delta=-75.9$ ppm (s); HR-MS (ESI) calcd for $[M-NTf_2]^+$ $C_{28}H_{41}Au_2F_6N_2O_4P_2S_2$ *m/z*: 1103.1218, found 1103.1210; elemental analysis calcd for $C_{30}H_{41}Au_2F_{12}N_3O_8P_2S_4$: C 26.04, H 2.99, N 3.04; C 26.38, H 3.68, N 2.79.

Complex 7-Ph: A vial was charged with **PN^{H}P^{Ph}**Au_2Cl_2 (50.2 mg, 0.05 mmol) and $AgNTf_2$ (38.8 mg, 0.10 mmol). Then, 5 mL CH_2Cl_2 was added and the resulting suspension was stirred for 1.75 h, during which time it colored purple. The mixture was filtered over Celite and the colorless filtrate was concentrated under removed pressure, leaving **7-Ph** as an off-white solid in high yield (66 mg, 87%). ^{1}H NMR (400 MHz, CD_2Cl_2): $\delta=7.60$ (dd, $J=8.5$, 6.2 Hz, 2H), 7.50 (td, $J=7.8$, 2.8 Hz, 4H), 7.44–7.16 (m, 16H), 7.13 (dd, $J=8.3$, 5.9 Hz, 2H), 6.42 (dd, $J=13.4$, 1.9 Hz, 2H), 4.95 (s, 1H), 2.16 ppm (s, 6H); ^{31}P{^{1}H} NMR (162 MHz, CD_2Cl_2): $\delta=17.6$ ppm (s); ^{13}C{^{1}H} NMR (101 MHz, CD_2Cl_2): $\delta=145.4$ (d, $J=8.2$ Hz), 135.5 (d, $J=2.4$ Hz), 135.4 (d, $J=14.4$ Hz), 134.9 (d, $J=10.1$ Hz), 134.1 (d, $J=7.2$ Hz), 133.2 (s), 133.1 (d, $J=8.5$ Hz), 130.4 (d, $J=12.4$ Hz), 129.9 (d, $J=12.6$ Hz), 127.2 (d, $J=68.4$ Hz), 126.1 (d, $J=67.0$ Hz), 125.1 (d, $J=6.8$ Hz), 119.7 (q, $J=323.4$ Hz), 117.7 (s), 117.1 (s), 20.9 ppm (s); ^{19}F NMR (282 MHz, CD_2Cl_2): $\delta=-75.4$ ppm (s); HR-MS (ESI) calcd for $[M-NTf_2]^+$ $C_{40}H_{33}Au_2F_6N_2O_4P_2S_2$ *m/z*: 1239.0592, found 1239.0624.

Single crystal X-ray crystallography: All reflection intensities for **6** and **7** were measured at 110(2) K using a SuperNova diffractometer (equipped with Atlas detector) with Mo ($\lambda=0.71073$ Å, compound **7**) or Cu $K\alpha$ radiation ($\lambda=1.54178$ Å, compound **6**) under the program CrysAlisPro (Versions 1.171.36.32 or 1.171.37.33 Agilent Technologies, 2014). The same program was used to refine the cell dimensions and for data reduction. The structure was solved with the program SHELXS-2014/7 (Sheldrick, 2015) and was refined on F^2 with SHELXL-2014/7 (Sheldrick, 2015). Analytical numeric absorption correction based on a multifaceted crystal model was applied

using CrysAlisPro for **6**. Numerical absorption correction based on Gaussian integration over a multifaceted crystal model was applied using CrysAlisPro for **7**. The temperature of the data collection was controlled using the system Cryojet (manufactured by Oxford Instruments). The H-atoms were placed at calculated positions using the instructions AFIX 13, AFIX 23, AFIX 43, or AFIX 137 with isotropic displacement parameters having values 1.2 or 1.5 *U*eq of the attached C atoms. For **7**, the H-atom attached to N1 was found from difference Fourier maps, and its coordinates were refined freely. The N–H distance was restrained to be 0.88(3) Å using the DFIX instruction. Additional details for **6**: The structure is partly disordered. The asymmetric unit contains two crystallographically independent Au–Au complexes (labelled A and B), and three NTf_2^- counterions. Two of the three anions are found at sites of inversions symmetry, and their occupancy factors are fixed at 0.5. The Au–Au complexes are ordered, whereas all anions are found disordered over two orientations. The occupancy factor of the major component of the anion found at no special position refines to 0.518(4). The crystal is non-merohedrally twinned, and two twin components could be isolated. The twin relationship corresponds to a two-fold axis along the reciprocal vector 0.2444a* + 0.9697b* + 0.0022c*. The BASF scale factor refines to 0.3026(18). Additional details for **7**: the structure is partly disordered. The asymmetric unit contains one disordered pentane lattice solvent molecule. The occupancy factor of the major component of the disorder refines to 0.801(11). The absolute configuration was established by anomalous-dispersion effects in diffraction measurements on the crystal, and the Flack parameter refines to −0.009(4).

Details for 6: $C_{28}H_{40}Au_2Cl_4F_6N_2O_4P_2S_2$, Fw = 1244.41, yellow plate, 0.18 × 0.15 × 0.03 mm, triclinic, $P\bar{1}$(No: 2), a = 14.7894(5), b = 16.1787(6), c = 16.9926(6) Å, α = 89.310(3), β = 89.008(3), γ = 73.238(3)°, V = 3892.4(2) Å^3, Z = 4, D_x = 2.123 g cm^{-3}, μ = 18.863 mm^{-1}. 40 254 Reflections were measured up to a resolution of (sin $\theta/\lambda)_{max}$ = 0.62 Å^{-1}. 16 875 Reflections were unique (R_{int} = 0.0389), of which 11 951 were observed [$I > 2\sigma(I)$]. 1169 parameters were refined with 890 restraints. $R1$/w$R2$ [$I > 2\sigma(I)$]: 0.0513/0.1367. $R1$/w$R2$ [all refl.]: 0.0670/0.1471. S = 0.934. Residual electron density between −3.85 and 2.73 e Å^{-3}.

Details for 7. $C_{30}H_{41}Au_2F_{12}N_3O_8P_2S_4{\cdot}C_5H_{12}$, Fw = 1455.91, colorless block, 0.41 × 0.29 × 0.27 mm, monoclinic, *Cc* (No: 9), a = 15.2255(4), b = 20.5320(4), c = 17.6351(5) Å, β = 112.891(3)°, V = 5078.7(2) Å^3, Z = 4, T = 110(2) K, λ = 0.71073 (Mo K-α), D_x = 1.904 g cm^{-3}, μ = 6.090 mm^{-1}. 19 707 Reflections were measured up to a resolution of (sin $\theta/\lambda)_{max}$ = 0.65 Å^{-1}. 7986 reflections were unique (R_{int} = 0.0262), of which 7757 were observed [$I > 2\sigma(I)$]. 652 Parameters were refined with 136 restraints. $R1$/w$R2$ [$I > 2\sigma(I)$]: 0.0186/0.0358. $R1$/w$R2$ [all refl.]: 0.0196/0.0363. S = 0.999. Residual electron density between −0.86 and 1.34 e Å^{-3}.

CCDC 1505947 (**6**) and 1505946 (**7**) contain the supplementary crystallographic data for this paper. These data are provided free of charge by The Cambridge Crystallographic Data Centre

Acknowledgements

This research was funded by the European Research Council (ERC) through Starting Grant 279097 (*EuReCat*) to J.I.v.d.V. Ed Zuidinga is acknowledged for skillful mass spectrometric analyses and Dr. Marc Devillard for useful tips and tricks on gold coordination chemistry.

Conflict of interest

The authors declare no conflict of interest.

Keywords: bimetallic systems · bridging ligand · C–H activation · gold · reactive ligand

[1] a) A. S. K. Hashmi, *Acc. Chem. Res.* **2014**, *47*, 864 – 876; b) M. Chiarucci, M. Bandini, *Beilstein J. Org. Chem.* **2013**, *9*, 2586 – 2614; c) B. Ranieri, I. Escofet, A. M. Echavarren, *Org. Biomol. Chem.* **2015**, *13*, 7103 – 7118; d) R. Dorel, A. M. Echavarren, *Chem. Rev.* **2015**, *115*, 9028 – 9072; e) Y. Wei, M. Shi, *ACS Catal.* **2016**, *6*, 2515 – 2524; f) D. Pflästerer, A. S. K. Hashmi, *Chem. Soc. Rev.* **2016**, *45*, 1331 – 1367.

[2] a) F. Rekhroukh, L. Estevez, S. Mallet-Ladeira, K. Miqueu, A. Amgoune, D. Bourissou, *J. Am. Chem. Soc.* **2016**, *138*, 11920 – 11929; b) M. Joost, A. Amgoune, D. Bourissou, *Angew. Chem. Int. Ed.* **2015**, *54*, 15022 – 15045; *Angew. Chem.* **2015**, *127*, 15234 – 15258; c) M. Joost, L. Estévez, K. Miqueu, A. Amgoune, D. Bourissou, *Angew. Chem. Int. Ed.* **2015**, *54*, 5236 – 5240; *Angew. Chem.* **2015**, *127*, 5325 – 5329; d) M. Joost, A. Zeineddine, L. Estévez, S. Mallet-Ladeira, K. Miqueu, A. Amgoune, D. Bourissou, *J. Am. Chem. Soc.* **2014**, *136*, 14654 – 14657; e) J. Guenther, S. Mallet-Ladeira, L. Estevez, K. Miqueu, A. Amgoune, D. Bourissou, *J. Am. Chem. Soc.* **2014**, *136*, 1778 – 1781; f) C.-Y. Wu, T. Horibe, C. Borch Jacobsen, F. D. Toste, *Nature* **2015**, *517*, 449 – 454; g) M. D. Levin, F. D. Toste, *Angew. Chem. Int. Ed.* **2014**, *53*, 6211 – 6215; *Angew. Chem.* **2014**, *126*, 6325 – 6329; h) J. Serra, C. J. Whiteoak, F. Acuña-Parés, M. Font, J. M. Luis, J. Lloret-Fillol, X. Ribas, *J. Am. Chem. Soc.* **2015**, *137*, 13389 – 13397; i) J. Serra, T. Parella, X. Ribas, *Chem. Sci.* **2017**, *8*, 946 – 952.

[3] a) H. Yang, T.-P. Lin, F. P. Gabbaï, *Organometallics* **2014**, *33*, 4368 – 4373; b) H. Yang, F. P. Gabbaï, *J. Am. Chem. Soc.* **2015**, *137*, 13425 – 13432; c) J. S. Jones, F. P. Gabbaï, *Chem. Lett.* **2016**, *45*, 376 – 384; d) L. Hettmanczyk, S. Manck, C. Hoyer, S. Hohloch, B. Sarkar, *Chem. Commun.* **2015**, *51*, 10949 – 10952; e) L. Hettmanczyk, L. Suntrup, S. Klenk, C. Hoyer, B. Sarkar, *Chem. Eur. J.* **2017**, *23*, 576 – 585; f) D. L. J. Broere, D. K. Modder, E. Blokker, M. A. Siegler, J. I. van der Vlugt, *Angew. Chem. Int. Ed.* **2016**, *55*, 2406 – 2410; *Angew. Chem.* **2016**, *128*, 2452 – 2456.

[4] Reviews and highlights: a) D. L. J. Broere, R. Plessius, J. I. van der Vlugt, *Chem. Soc. Rev.* **2015**, *44*, 6886 – 6915; b) O. R. Luca, R. H. Crabtree, *Chem. Soc. Rev.* **2013**, *42*, 1440 – 1459; c) R. F. Munhá, R. A. Zarkesh, A. F. Heyduk, *Dalton Trans.* **2013**, *42*, 3751 – 3766; d) V. K. K. Praneeth, M. R. Ringenberg, T. R. Ward, *Angew. Chem. Int. Ed.* **2012**, *51*, 10228 – 10234; *Angew. Chem.* **2012**, *124*, 10374 – 10380; e) J. I. van der Vlugt, *Eur. J. Inorg. Chem.* **2012**, 363 – 375; f) V. Lyaskovskyy, B. de Bruin, *ACS Catal.* **2012**, *2*, 270 – 279; g) W. I. Dzik, X. P. Zhang, B. de Bruin, *Inorg. Chem.* **2011**, *50*, 9896 – 9903; h) W. Kaim, *Inorg. Chem.* **2011**, *50*, 9752 – 9765; i) W. I. Dzik, J. I. van der Vlugt, J. N. H. Reek, B. de Bruin, *Angew. Chem. Int. Ed.* **2011**, *50*, 3356 – 3358; *Angew. Chem.* **2011**, *123*, 3416 – 3418.

[5] Recent examples: a) B. Bagh, D. L. J. Broere, V. Sinha, P. F. Kuijpers, N. P. van Leest, B. de Bruin, S. Demeshko, M. A. Siegler, J. I. van der Vlugt, *J. Am. Chem. Soc.* **2017**, *139*, doi: 10.1021/jacs.7b00270; b) B. Bagh, D. L. J. Broere, M. A. Siegler, J. I. van der Vlugt, *Angew. Chem. Int. Ed.* **2016**, *55*, 8381 – 8385; *Angew. Chem.* **2016**, *128*, 8521 – 8525; c) D. L. J. Broere, N. P. van Leest, B. de Bruin, M. A. Siegler, J. I. van der Vlugt, *Inorg. Chem.* **2016**, *55*, 8603 – 8611; d) J. Jacquet, P. Chaumont, G. Gontard, M. Orio, H. Vezin, S. Blanchard, M. Desage-El Murr, L. Fensterbank, *Angew. Chem. Int. Ed.* **2016**, *55*, 10712 – 10716; *Angew. Chem.* **2016**, *128*, 10870 – 10874; e) D. L. J. Broere, D. K. Modder, E. Blokker, M. A. Siegler, J. I. van der Vlugt, *Angew. Chem. Int. Ed.* **2016**, *55*, 2406 – 2410; *Angew. Chem.* **2016**, *128*, 2452 – 2456; f) A. Ali, S. K. Barman, R. Mukherjee, *Inorg. Chem.* **2015**, *54*, 5182 – 5194; g) C. C. Comanescu, M. Vyushkova, V. Iluc, *Chem. Sci.* **2015**, *6*, 4570 – 4579; h) D. L. J. Broere, M. A. Siegler, J. I. van der Vlugt, *Angew. Chem. Int. Ed.* **2015**, *54*, 1516 – 1520; *Angew. Chem.* **2016**, *127*, 1536 – 1540; i) J. Jacquet, E. Salanouve, M. Orio, H. Vezin, S. Blanchard, E. Derat, M. Desage-El Murr, L. Fensterbank, *Chem. Commun.* **2014**, *50*, 10394 – 10397; j) M. van der Meer, Y. Rechkemmer, I. Peremykin, S. Hohloch, J. van Slageren, B. Sarkar, *Chem. Commun.* **2014**, *50*, 11104 – 11106; k) Z. Alaji, E. Safaei, L. Chiang, R. M. Clarke, C. Mu, T. Storr, *Eur. J. Inorg. Chem.* **2014**, 6066 – 6074; l) C. A. Sanz, M. J. Ferguson, R.

McDonald, B. O. Patrick, R. G. Hicks, *Chem. Commun.* **2014**, *50*, 11676 – 11678; m) W. Zhou, B. O. Patrick, K. M. Smith, *Chem. Commun.* **2014**, *50*, 9958 – 9960; n) M.-C. Chang, T. Dann, D. P. Day, M. Lutz, G. G. Wildgoose, E. Otten, *Angew. Chem. Int. Ed.* **2014**, *53*, 4118 – 4122; *Angew. Chem.* **2014**, *126*, 4202 – 4206; o) J. L. Wong, R. H. Sánchez, J. C. Logan, R. A. Zarkesh, J. Ziller, A. F. Heyduk, *Chem. Sci.* **2013**, *4*, 1906 – 1910; p) D. L. J. Broere, B. de Bruin, J. N. H. Reek, M. Lutz, S. Dechert, J. I. van der Vlugt, *J. Am. Chem. Soc.* **2014**, *136*, 11574 – 11577; q) T. W. Myers, L. A. Berben, *Chem. Commun.* **2013**, *49*, 4175 – 4177; r) K. Ouch, M. S. Mashuta, C. A. Grapperhaus, *Inorg. Chem.* **2011**, *50*, 9904 – 9914; s) A. L. Smith, K. I. Hardcastle, J. D. Soper, *J. Am. Chem. Soc.* **2010**, *132*, 14358 – 14360; t) S. D. J. McKinnon, B. O. Patrick, A. B. P. Lever, R. G. Hicks, *Chem. Commun.* **2010**, *46*, 773 – 775; u) K. J. Sylvester, P. J. Chirik, *J. Am. Chem. Soc.* **2009**, *131*, 8772 – 8774; v) M. Königsmann, N. Donati, D. Stein, H. Schönberg, J. Harmer, A. Sreekanth, H. Grützmacher, *Angew. Chem. Int. Ed.* **2007**, *46*, 3567 – 3570; *Angew. Chem.* **2007**, *119*, 3637 – 3640.

[6] A. I. Olivos Suarez, V. Lyaskovskyy, J. N. H. Reek, J. I. van der Vlugt, B. de Bruin, *Angew. Chem. Int. Ed.* **2013**, *52*, 12510 – 12529; *Angew. Chem.* **2013**, *125*, 12740 – 12760.

[7] A. T. Radosevich, J. G. Melnick, S. A. Stoian, D. Bacciu, C. H. Chen, B. M. Foxman, O. V. Ozerov, D. G. Nocera, *Inorg. Chem.* **2009**, *48*, 9214 – 9221.

[8] D. Adhikari, S. Mossin, F. Basuli, J. C. Huffman, R. K. Szilagyi, K. Meyer, D. J. Mindiola, *J. Am. Chem. Soc.* **2008**, *130*, 3676 – 3682.

[9] V. Vreeken, M. A. Siegler, B. de Bruin, J. N. H. Reek, M. Lutz, J. I. van der Vlugt, *Angew. Chem. Int. Ed.* **2015**, *54*, 7055 – 7059; *Angew. Chem.* **2015**, *127*, 7161 – 7165.

[10] S. B. Harkins, N. P. Mankad, A. J. M. Miller, R. K. Szilagyi, J. C. Peters, *J. Am. Chem. Soc.* **2008**, *130*, 3478 – 3485.

[11] V. Vreeken, D. L. J. Broere, A. C. H. Jans, M. Lankelma, J. N. H. Reek, M. A. Siegler, J. I. van der Vlugt, *Angew. Chem. Int. Ed.* **2016**, *55*, 10042 – 10046; *Angew. Chem.* **2016**, *128*, 10196 – 10200.

[12] A further notable attribute of complex **2** is the μ-Cl ligand bridging the two Au-centers, which is an uncommon motif: a) A. Grirrane, E. Álvarez, H. García, A. Corma, *Angew. Chem. Int. Ed.* **2014**, *53*, 7253 – 7258; *Angew. Chem.* **2014**, *126*, 7381 – 7386; b) N. Phillips, T. Dodson, R. Tirfoin, J. I. Bates, S. Aldridge, *Chem. Eur. J.* **2014**, *20*, 16721 – 16731; c) A. Homs, I. Escofet, A. M. Echavarren, *Org. Lett.* **2013**, *15*, 5782 – 5785; d) V. W.-W. Yam, C.-L. Chan, K.-K. Cheung, *J. Chem. Soc. Dalton Trans.* **1996**, 4019 – 4022; e) P. G. Jones, G. M. Sheldrick, R. Uson, A. Lapuna, *Acta Crystallogr. Sect. B* **1980**, *36*, 1486 – 1488; f) Dimeric structures: A. Hamel, N. W. Mitzel, H. Schmidbaur, *J. Am. Chem. Soc.* **2001**, *123*, 5106 – 5107.

[13] N. G. Connelly, W. E. Geiger, *Chem. Rev.* **1996**, *96*, 877 – 910. Also the reduction of **1** is irreversible under these electrochemical conditions.

[14] K. Zhang, J. Prabhavathy, J. H. K. Yip, L. L. Koh, G. K. Tan, J. J. Vittal, *J. Am. Chem. Soc.* **2003**, *125*, 8452 – 8453.

[15] Y. Zhu, C. S. Day, L. Zhang, K. J. Hauser, A. C. Jones, *Chem. Eur. J.* **2013**, *19*, 12264 – 12271.

[16] D. Wang, R. Cai, S. Sharma, J. Jirak, S. K. Thummanapelli, N. G. Akhmedov, H. Zhang, X. Liu, J. L. Petersen, X. Shi, *J. Am. Chem. Soc.* **2012**, *134*, 9012 – 9019.

[17] The structure of **6** (and that of **1**) contains one C–H bond of one phenyl ring being eclipsed by the π-system of the second phenyl ring. We propose that this particular geometry in **6** pre-organizes the C–H bond for oxidative activation to form the C–C bond. The double C–H activation of the ligand backbone could proceed by formation of an *ortho*-phenyl radical (see Scheme 1; potentially by initial generation of a diarylamido radical cation) upon abstraction of this hydrogen as an H-atom, followed by coupling with the second phenyl ring. However, we so far do not have experimental data to elaborate on this part of the transformation in more detail.

[18] L. Fan, B. M. Foxman, O. V. Ozerov, *Organometallics* **2004**, *23*, 326 – 328.

[19] J. D. Masuda, K. C. Jantunen, O. V. Ozerov, K. J. T. Noonan, D. P. Gates, B. L. Scott, J. L. Kiplinger, *J. Am. Chem. Soc.* **2008**, *130*, 2408 – 2409.

[20] J. Yu, C. Zhang, *Synthesis* **2009**, 2324 – 2328.

Manuscript received: January 24, 2017

Accepted Article published: March 1, 2017

Final Article published: April 3, 2017

